

# **Development of an Ultra-Sensitive Spectrometer**



**LUND**  
**UNIVERSITY**

**Master Thesis**

**Sukant Chaudhry**

**Supervisors - Elias Kristensson  
Joakim Bood**

**Division of Combustion Physics at Lund University**

**May 2016**

## Abstract

A high dynamic range imaging (HDRI) spectroscopic instrument was designed and developed in this thesis. Achieving higher measurement accuracy in imaging spectroscopic measurements require both a suppression of the background light (stray light) as well as HDR imaging. A Digital Micromirror Device (DMD), which spatially modulates the light, was employed in the designed spectrometer to produce HDRI and the Periodic Shadowing technique was used for stray light elimination. A Czerny-Turner spectrometer was designed and developed, having a grid pattern at the entrance slit to enable Periodic Shadowing. The DMD was introduced at the output of the spectrometer, which allowed a desired percentage of the spectral lines to be reflected onto the detector. This made it possible to resolve weak spectral lines in the presence of intense ones at one exposure time, without saturating the camera. Experimental results are provided to demonstrate the capabilities of the device and the HDRI achieved. This instrument holds promise for improved Raman scattering spectroscopy, which currently is restricted by both stray light and a limited dynamic range.

## Acknowledgment

This thesis project was done at the Combustion Physics division of Lund University as a partial requirement for fulfillment of my master education in Photonics and would not have been possible without the kindly help of several persons. First of all, I would like to thank my supervisor Elias Kristensson for providing me the opportunity to do the master project, always encouraging me to think through the step by step planning and designing process for the project. He has always been willing to answer the questions with a welcoming and positive attitude and also supervising me and guiding me in the lab whenever possible. Secondly, I would like to thank Per-Erik Bengtsson and Joakim Bood for helping me find the best suitable project. I would like to thank Eduourd Berrocal for always being helpful and insightful with the discussions. I would also like to thank all the other group members for their warm friendly welcome and support. The software Inkscape was used for the drawings in my thesis report and I would like to acknowledge Alexander Franzen for developing the component library. Finally, I would like to thank my parents, twin sister, brother and my girlfriend for giving me firm support throughout my masters.

## List of Abbreviations

DMD	Digital Micromirror Device
HDR	High Dynamic Range
PS	Periodic Shadowing
DSLR	Digital single-lens reflex
RGB	Red- Green- Blue
SLM	Spatial Light Modulator
TIR	Total Internal Reflection
CW	Continuous wave

# Table of Contents

<b>1.Introduction</b> .....	<b>1</b>
<b>2.Theory</b> .....	<b>3</b>
2.1 Czerny-Turner Spectrometer .....	3
2.2 Resolution of Spectrometer .....	5
2.3 Error in Spectroscopic measurements .....	5
2.4 Periodic shadowing.....	6
2.5 High Dynamic Range Imaging .....	6
2.6 Digital Micromirror Device (DMD).....	6
2.7 Total Internal Reflection (TIR).....	8
2.8 Scheimpflug Principle .....	9
<b>3.Method</b> .....	<b>11</b>
3.1 Optical Design .....	11
3.2 Alignment of the Spectrometer.....	13
3.3 Recording spectrum with Periodic Shadowing.....	16
3.4 Digital Micromirror Device (DMD) experiment to achieve High Dynamic Range Imaging .....	19
3.4.1 Tracing the ON and OFF state reflection and controlling a micromirror's flip .....	19
3.4.2 Experimental Challenges .....	19
<b>4.Result and Discussions</b> .....	<b>23</b>
4.1 Intensity control using the DMD .....	23
4.2 HDR image achieved with PS .....	24
<b>5.Conclusion and Outlook</b> .....	<b>28</b>
<b>References</b> .....	<b>29</b>

# 1. Introduction

Nearly all fields within natural science employ optical spectroscopy to study the absorption and emission of light, relating to the characteristics of the sample using radiation. The wavelength (color) emitted or absorbed by a substance provides insight to the molecular composition of the sample, as well as other important properties (temperature, pressure, *etc.*). Spectroscopic information and analysis has played an important role in the development of the most fundamental theories in physics. Optical spectroscopic techniques have wide applications varying from two-dimensional (2D) spectroscopy of nuclear magnetic resonance (NMR), nonlinear optical spectroscopy [1] to medical field for detection of tumors [2]. Moreover, it has applications extending from solid state research of optical characterization of quantum dots in nanowire, to various optical spectroscopic techniques used for combustion research.

One common problem in spectroscopy is that it is very difficult to resolve a weak spectral signal in presence of a high intense spectral signal, analogous to observing e.g. a comet orbiting the sun. However, by blocking the sun with your hand, the comet may be observed. This is the idea implemented in the designing of an ‘Ultra-sensitive spectrometer’, by using a Digital Micromirror Device (DMD) in the so-called Czerny-Turner configuration with the aim to achieve a high dynamic range (HDR) spectroscopic instrument. A DMD modulates the light signal in the spatial domain and has a chip which consists of more than a million micrometer-sized mirrors arranged in a rectangular array. Each mirror in the array has an ability to flip in +12 degrees and -12 degrees (ON and OFF states). The DMD makes it possible to achieve a situation where all spectral components have equal intensities, by only reflecting a small percentage of the high intense lines, and a large percentage of the weak ones in the spectrum, thereby boosting the dynamic range.

Moreover, a common measurement obstacle in spectroscopy is the interference from the unwanted signal reaching the detector in unintended ways known as stray light, which causes spectral distortion and in severe situations, leads to the inability to detect spectral lines. To correct for this issue, a technique called ‘periodic shadowing’ is implemented in the designed spectrometer [3]. This technique effectively suppresses the stray light by implementing a grid pattern at the entrance of the spectrometer. The grid pattern tags the photons entering the spectrometer. Inside the spectrometer, only the ‘signal photons’ maintain the periodic pattern, whereas the background light (arising from scattering inside the spectrometer) loses it. Using a spatial lock-in algorithm, the signal photons can be extracted while eliminating the background or stray light.

One typical spectroscopic application for the instrument described in this thesis is Raman scattering spectroscopy, commonly used for molecular determination. Raman scattering is a relatively weak process and often the spectral lines appear near the  $\sim 1000$  times stronger laser line (Rayleigh scattering, stemming from elastic scattering). The intense laser line tends to ‘bleed’ into the weaker Raman lines, making them very difficult to resolve.

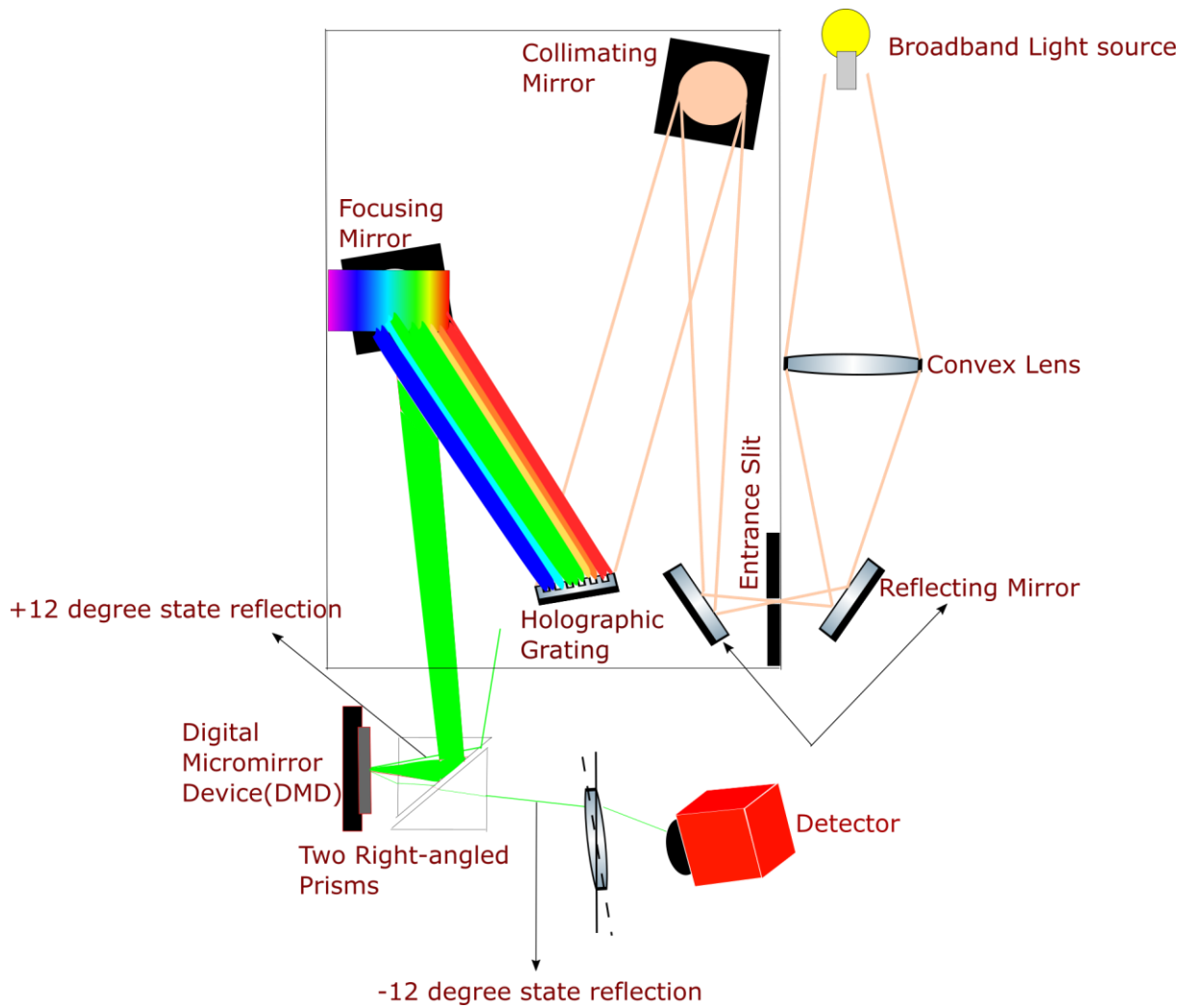


*Figure 1: Final design of the DMD spectrometer. Spectral component of incident light from lamp falls in focus on DMD chip. DMD chip reflects it in ON and OFF state, and these paths are separated using two right angled prisms. The imaging is done using Scheimpflug Principle.*

## 2. Theory

### 2.1 Czerny-Turner Spectrometer

A Cadmium spectral lamp is used as the light source in spectrometer, emitting light in all directions. A positive spherical lens is used to collect a portion of the emitted light and image it onto the entrance slit, based on the lens-makers formula:

$$1/Z_1 + 1/Z_2 = 1/F \quad (1)$$

where  $Z_1$  is the distance between the lens plane and the light source,  $Z_2$  is the distance at which the image is formed from the lens plane and  $F$  is the focal length of the lens [4]. If the distance  $Z_1$  is equal to  $2F$ , the image is formed at a distance  $2F$  from the lens plane as well, with a magnification of 1:1. The entrance slit is an essential part of the spectrometer as it controls the amount of light (photon flux) entering the spectrometer. Decreasing its width will give better spectral resolution (sharper spectral lines at the detector) but at the expense of signal strength.

A dispersive element – often a prism or a diffraction grating – inside spectrometer will disperse the collected light into its spectral components. The dispersion caused by a prism is wavelength dependent; increasing strongly towards shorter wavelengths and decreasing at longer wavelengths, making the spectral resolution wavelength-dependent [5]. There are two types of diffraction gratings, either ruled- or holographic gratings. The major difference between the two is the manufacturing process. Ruled gratings are created using an etching process, where a large number of parallel grooves are etched onto the surface of substrate which is coated with a highly reflective material. Holographic gratings, on the other hand, are formed via the interference of two crossed laser beams, which together create a sinusoidal index of refraction variation in a piece of optical glass [5]. Unlike grooved gratings, holographic ones can be made to either transmit or reflect light. Another benefit is that holographic gratings generate a lower level of diffusely scattered light. The number of lines  $N$  per millimeter scale defines the groove frequency, varying from hundreds to several thousand. Decreasing the spacing  $d$  between the lines on the grating surface will increase the groove frequency. As light illuminates the grating, a diffraction pattern is obtained which is basically the summation of diffraction from each grating line. The angular relationship between the incident and diffracted beam is given by the grating equation [6]:

$$m\lambda = d(\sin \Theta_i + \sin \Theta_o) \quad (2)$$

The equation reveals that the diffraction pattern consists of diffraction maxima ( $m$ ), occurring only at certain angles. A diffraction maximum is created when the differences in optical path length between diffracted wavefronts are integral multiple ( $m$ ) of wavelengths ( $\lambda$ ).  $m$  can have



values  $0, \pm n$ , where  $n$  is an integer value.  $\theta_i$  and  $\theta_o$  are the incident- and diffraction angles, respectively.

After entering the spectrometer, the collected light starts to diverge and, in the Czerny-Turner design, a concave mirror is used to collimate it. The collimation of light beams is an important step for the grating to diffract the beam into its spectral components. If the rays in the beam are not collimated, the diffraction created by the grating will consist of an irreversible mixing of the spectral components. The use of a mirror is also important, as lenses tend to have a focal length that is wavelength dependent. Collimation is achieved by placing the concave mirror at a distance equal to its focal length from the entrance slit [4]. The collimated beam of light uniformly illuminates the grating surface, which then is diffracted into its spectral components. A portion of the diffracted beam falls on a second concave mirror, focusing this parallel light to a point at a distance equal to the focal length of the mirror, effectively creating a 1:1 spectrally resolved image of the entrance slit [7]. By rotating the grating, the whole spectrum can be recorded.

For 2D spectroscopy, the charge coupled device (CCD) camera and the complementary metal-oxide semiconductor (CMOS) camera are most commonly used. The difference between these types of sensors lies in how they process the acquired data. In both cases, the light energy captured by the camera is sent to the image storage media. A 2D array consisting of tiny photodiodes records the light energy and converts it to an analog signal, which is sent to a voltage converter that creates the digital image. This formation of a digital image occurs in different ways for CMOS and CCD sensors [8]. One major difference is that each pixel on CMOS chip is processed using its individual charge-to-voltage converter, which tends to worsen the image quality. CCD cameras produce high quality images but are, in general, expensive compared to CMOS cameras [8]. CCD detectors are often preferred for spectroscopic applications in visible regimes, but in the near-infrared- and infrared regime they lose sensitivity. In the current experiment, a digital single-lens reflex (DLSR) camera is used, having advantages such as large digital image sensors, high pixel densities as well as allowing RGB (red, blue and green) pictures to be captured. Larger-sized image sensors allow more details to be captured, together with better dynamic range, less noise and improved light performance [9].

## 2.2 Resolution of a spectrometer

Spectral resolution is an essential characteristic of a spectrometer; specifying how good the spectrum is resolved. For example, if the bandwidth or wavelength range covered by the spectrometer is 100 nm with a spectral resolution of 1nm, implies that 100 spectral peaks can be resolved in the spectrum. The major factors affecting the resolution are spectrometer focal length, diffraction grating groove frequency, slit width, and detector.

- **Focal Length** –

The focal length in a Czerny-Turner spectrometer is the distance between the entrance slit and the collimating mirror and similarly the distance between the focusing mirror and the detector. When the focal length of the spectrometer is increased, the optical path length travelled by the light beams increases, which in turn gives less spectral overlap compared to a shorter focal length and thus better spectral resolution. With this increase in focal length, however, the incident light is spread over a larger area, resulting in a reduced signal level as the collimating mirror collects a relatively lower amount of light.

- **Diffraction Grating** –

Higher spectral resolution is achieved with the higher groove frequency of the diffraction grating. When the groove frequency is increased, the dispersion increases, providing better separation of the incident wavelengths. Thus, the spectrum is resolved more finely but there is a tradeoff with the spectral information obtained. Considering equation (2),  $\theta_o$  will be large for small spacing  $d$ , and thus the spectral range covered is limited.

## 2.3 Error in Spectroscopic measurements

Most spectroscopic techniques suffer from interference effects which are known as stray light error. Stray light is the unwanted signal arising due to scattering inside the spectrometer and reaches the detector in the unintended ways, which causes distortion of spectral lines, difficulties in resolving weak spectral lines and sometimes make it difficult to even detect the spectral lines in a spectrum [10]. Thus, this enhanced background due to stray light, worsens the spectral resolution, the detection limit, suppression of weak spectral features and give rise to calibration errors [11, 12, 13]. This enhanced background varies across the wavelength range of the spectrum, and increases vastly around strong intense lines. This local increase of stray light is because of the superposition of wings associated with the strong emission lines [3].

## 2.4 Periodic Shadowing

Period Shadowing (PS) is a technique, recently developed at the Combustion Physics department, Lund University that effectively suppresses the stray light errors without adding any significant experimental complexity. The suppression of enhanced background is achieved by putting a grid pattern at the entrance slit. This pattern is imposed on the incident photons and makes it possible to distinguish these tagged photons from the unwanted signal at the detector. This is possible because the unwanted stray light is incapable to maintain this well-defined pattern through the passage in the spectrometer. The fine strips of grid effectively cast periodic shadows (hence its name) of the pattern with a spatial frequency and phase along the slit direction onto the detector at all wavelengths. This makes it possible to extract the envelope of wanted signal and eliminate the unwanted signal using a lock-in algorithm [3].

## 2.5 High Dynamic Range Imaging

In imaging spectroscopic measurements, it is difficult to resolve less intense or weak spectral lines in presence of strong ones and this restricts the dynamic range of imaging. Increasing the exposure time of the detector will, however, lead to saturation. Thus, a detection limit primarily depends on stray light and dynamic range of the detector [14] and to improve this overall detection limit of a system either the actual signal can be boosted or the background noise can be reduced. Both of the aims are achieved at the same time by implementing a 'Digital Micromirror Device(DMD)' and performing periodic shadowing in the designed spectrometer.

## 2.6 Digital Micromirror Device (DMD)

A DMD is a chip that consists of more than a million micrometer sized mirrors arranged in a rectangular array, with an ability to flip each individual mirror to either a small positive angle (10 to 12 degrees in general) or to the respective negative angle. The DMD works as a spatial light modulator (SLM) [4], and modulates the light signals spatially or in time domain, which can be coupled to system to achieve amplitude, phase, and direction modulation of the incident light.

The DMD used in the project is DLP 0.95 1080p, seen in Figure 3, consisting of a 2,073,600 highly reflective, digitally switchable, micrometer sized (10.8  $\mu\text{m}$ ) mirrors, arranged in a 2D rectangular array of 1920 columns to 1080 rows giving 1080p resolution. A DMD pixel refers to each individual mirror, and can flip to either +12 degrees or -12 degrees, giving the ON and OFF state. By convention, the positive state is titled toward the illumination, referring to the ON state and negative state is tilted away from the illumination, referring to the OFF state. In general, the reflection path in which the detector is placed is referred as the ON state. The

tilting of the mirrors are perpendicular to an axis which is defined diagonally relative to the whole array of mirrors; 45 degrees with respect to the normal, as shown in Figure 2. This axis is known as the “hinge axis” and the position of the pixel in ON state (positive angle tilt) is towards left side (towards row 0 and column 0), and the position of pixel to reflect light in OFF state is towards right side of hinge axis.

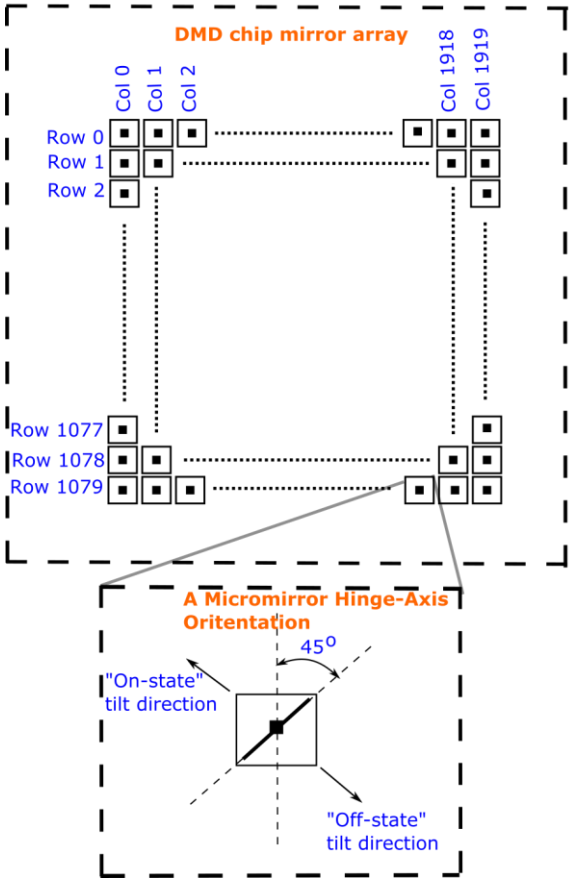


*Figure 2: DMD chip consisting of Micromirror array, and hinge-axis orientation.*

The DMD used in the experiment is seen in Figure 3, with different components labelled. The DMD chip is connected to the controller board circuit via two 12 inches flex cables, which transfer information from controller board to the DMD extension board. Both the DMD extension board and controller board have 4 small holes which are meant for mounting the device. DDR3 SO-DIMM component in controller board is a memory unit used to store data (picture) that can be uploaded on the DMD chip. There is a FPGA (field- programmable gate array) integrated in the circuit which converts the uploaded data (for example a picture) into a format that is readable by the DMD chip. There are cooling elements required to actively and passively cool the FPGA element.

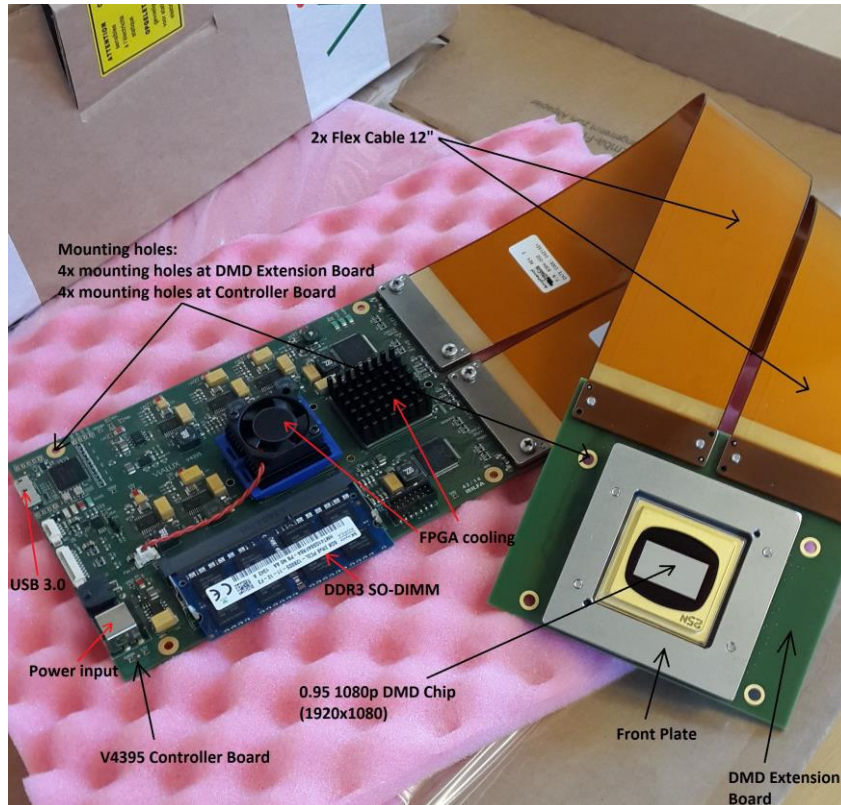


*Figure 3: DMD chip module.*

## 2.7 Total Internal Reflection(TIR)

The incident light rays travelling to a medium of a different refractive index are refracted at the boundary of the two media, and this angle of refraction can be calculated using Snell's law. This law relates the angle of refraction to the angle of incidence based on following equation (3) [4].

$$n_1 \sin \theta_1 = n_2 \sin \theta_2 \quad (3)$$

$n_1$  is the refractive index of the medium the incident light is travelling from and  $n_2$  is the refractive index of the medium, upon which incident light is incident.  $\theta_1$  is the angle of incidence and  $\theta_2$  is the angle of refraction. When the light rays are travelling from a medium of higher  $n_1$  to lower  $n_2$  for example, glass to air, the rays are refracted away from the normal at the boundary of the two mediums, as the angle of refraction will be greater than the angle of incidence. Increasing the angle of incidence eventual leads to a situation where the refraction angle equals 90 degrees. This is referred to the critical angle,  $\theta_C$ , calculated using equation (4) [4].

$$\theta_C = \sin^{-1} n_2/n_1. \quad (4)$$

As the angle of incidence further increases, Snell's law is no longer satisfied and no refraction occurs at the boundary. The rays are totally internally reflected in the medium and this phenomenon is called the 'Total internal reflection', observed in Figure 4. For example, when the light rays are travelling from reflective prism,  $n_1 > 1.4142$  to air,  $n_2 = 1$ , the critical angle is less than 45 degrees. Hence, all the rays with angle of incidence greater than  $\theta_c$ , will be totally internally reflected, shown in Figure 4.

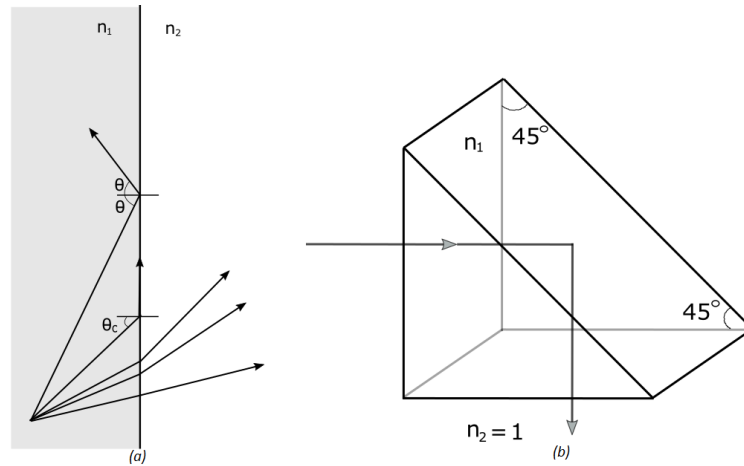


*Figure 4: (a)  $n_1$  is greater than  $n_2$ . Incident rays goes refracted along the boundary at 90 degree when angle of incidence is equal to critical angle. The incident rays are totally internally reflected when angle of incidence is greater than critical angle. (b) Light rays travelling from reflecting prism of glass material to air are totally internally reflected. [Adapted from Fundamental of Photonics, Chapter 1 Ray Optics, by B.E.A. Saleh, M.C. Teich, 2<sup>nd</sup> ed. (Wiley,2007)]*

## 2.8 Scheimpflug Principle

In imaging, to focus an entire object plane, it is an essential condition to have the object plane, the lens plane and the camera sensor plane all parallel to each other. The camera/detector can only focus a part of the object plane when the lens plane of the camera and object plane are not parallel. The Scheimpflug configuration is used to solve this problem, based on the Scheimpflug principle which states that a sharp focus can be achieved by tilting of the image sensor and lens with respect to each other such that image plane intersects with the both object and lens planes [15, 16]. When all of these three planes coincide at a point, the image will be in focus all along the image plane. However, it is seen in many applications that the magnification is not constant all along the image plane even when the image is in focus all along the image plane [17]. Figure 5 shows the object plane tilted or rotated, making an angle  $\theta$  with the lens plane. Based on this angle of inclination of the lens,  $\theta$ , the image plane has to be rotated or tilted accordingly at an angle  $\alpha$ , to get the entire object plane in focus, which can be calculated using the relation in equation (5) [15].

$$\tan \alpha / \tan \theta = M \quad (5)$$

Here,  $M$  is the magnification of the object plane desired.

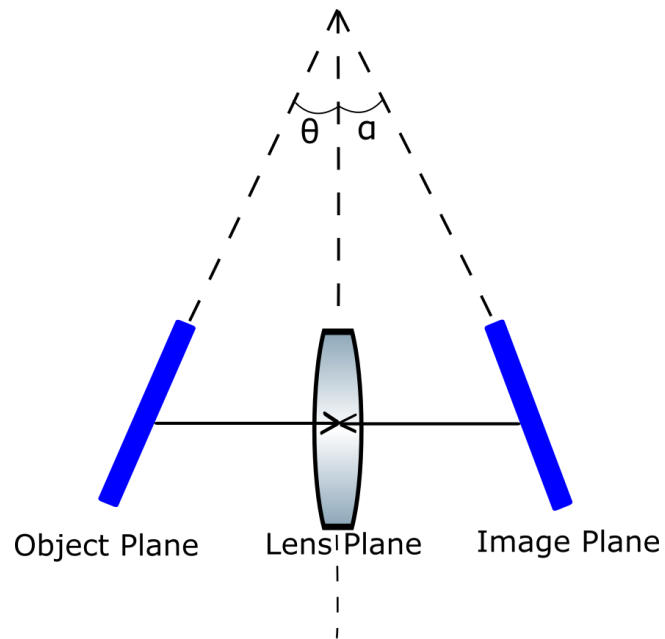


*Figure 5: Scheimpflug intersection to obtain the entire object plane in focus.*

## 3. Method

### 3.1 Optical Design

A Czerny-Turner spectrometer design is selected as it presents several benefits, such as 2D capabilities, low experimental complexity and wavelength scanning flexibility. Moreover, as this design is entirely based on reflection, it is naturally achromatic. A Czerny-Turner spectrometer of focal length 700 mm was designed in the FRED, which is an Optical Engineering Software for ray tracing, seen in Figure 6.

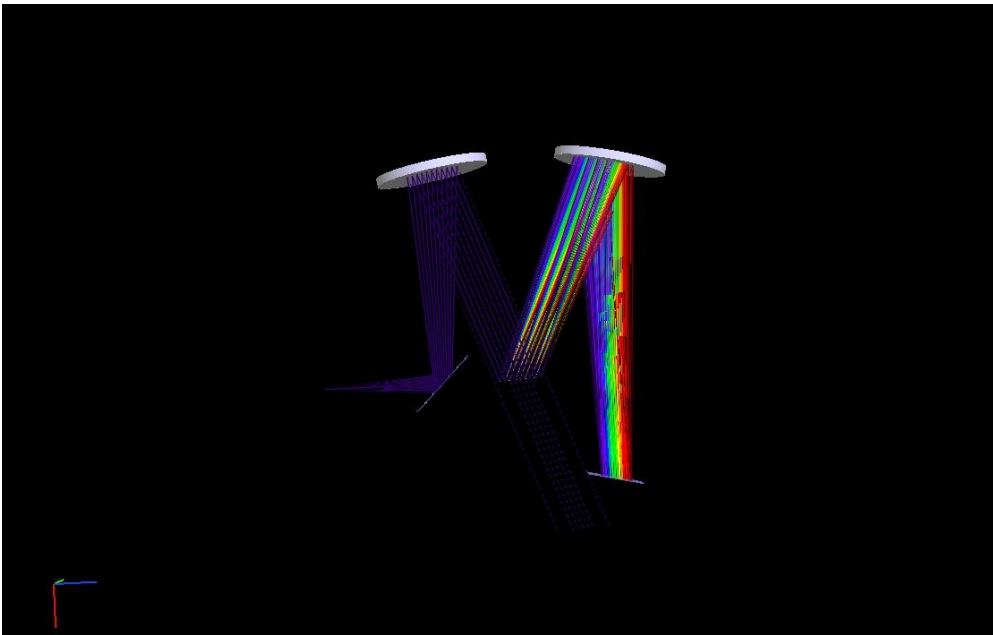


*Figure 6: A Czerny-Turner Spectrometer of 700 mm focal length.*

The best resolution obtained with this focal length was 4 nm and Figure 7 shows a comparison of the resolving of spectral peaks obtained with the change of the focal length, from 700 mm to 400 mm, while keeping all other parameters the same. When the focal length is higher, the peaks are well resolved and none of the peaks are resolved when the focal length is reduced to 400 mm.



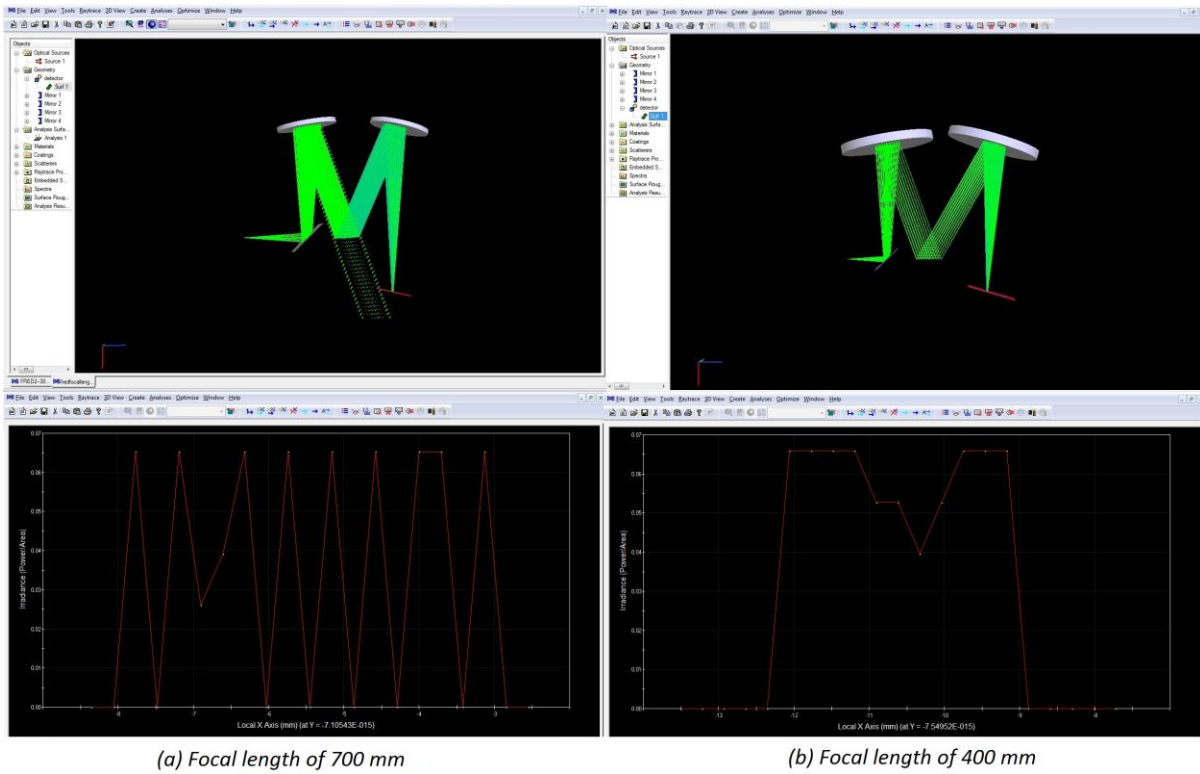


**Figure 7:** Comparison of peaks resolved in case of (a) Focal length of 700 mm and (b) Focal length of 400 mm.

A broadband Cadmium emission lamp was used as a light source and it was imaged at the entrance slit using a convex lens of focal length of 150 mm, as shown in Figure 8. The entrance slit was positioned at a distance equal to the focal length of the collimating mirror (762 mm) from the collimating mirror. This collimated light was directed onto the grating surface which disperses the incoming light into its different color components. The part of the dispersed light falling onto the focusing mirror aperture are focused at a distance equal to its focal length and at this position the detector (SLR camera) was placed.



*Figure 8: (a) Image formation of spectral lamp at the entrance slit. The collimating mirror was placed at a focal length distance from the slit. The Green horizontal line representing the height of the focal plane defined inside the spectrometer. (b) Side view to show the diffraction grating, collimating and focusing mirror, focusing the 0<sup>th</sup> order and first order diffraction.*

### 3.2 Alignment of the Spectrometer

Aligning of the spectrometer is an important step to e.g. ensure that the diffracted spectral lines of every order reach the detector plane at the same height. This process involves defining a certain height that the rays travel at throughout their passage inside the spectrometer, marked with a green horizontal small line in Figure 8(a).

This task was performed using a Continuous Wave (CW) laser source and it was positioned at a height in the center of the collimating and focusing mirror. Before introducing the laser beam into the spectrometer, the height of it is controlled over a long distance, to ensure that it is horizontal. An aperture corresponding to this height was set, and all other optical elements were adjusted accordingly. When the laser beam hits the grating surface, the light was reflected in three directions. The zeroth order, which is not refracted but reflected, and the two

+/-1 diffraction orders on either side of the zeroth order. It is advised to monitor these reflections in far field, making it easy to adjust both simultaneously. Figure 9 shows how both the +/-1 orders were monitored together at separate walls.

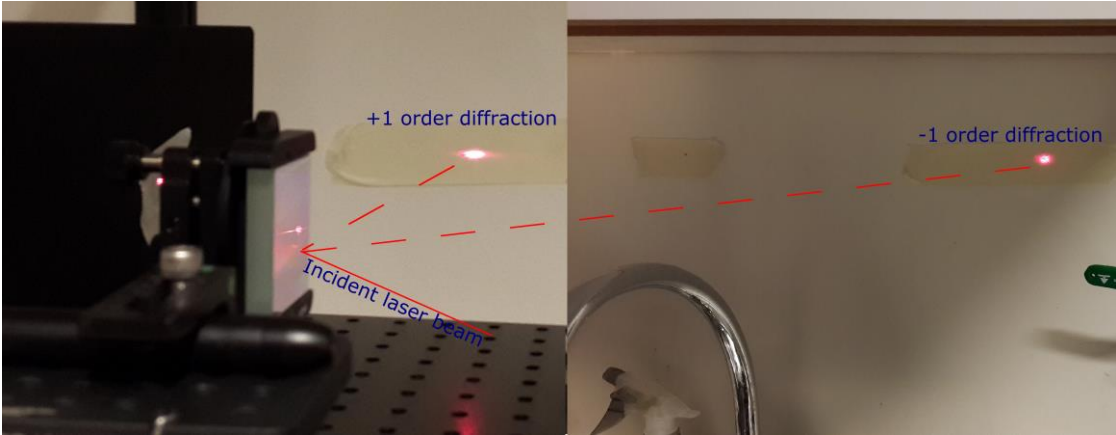


*Figure 9: +1 and -1 order diffractions from grating monitored simultaneously to align them at desired height.*

Note that a grating with a lower groove frequency generates a higher number of orders. Aligning each order reflection at a same height focal plane was achieved by rotating and tilting of the grating.

The tilting of grating in the forward or backwards direction moves the +1 and -1 reflections together downwards or upwards, respectively. The effect of rotation of the grating sideways in clockwise and anti-clockwise direction can be seen in Figure 10.

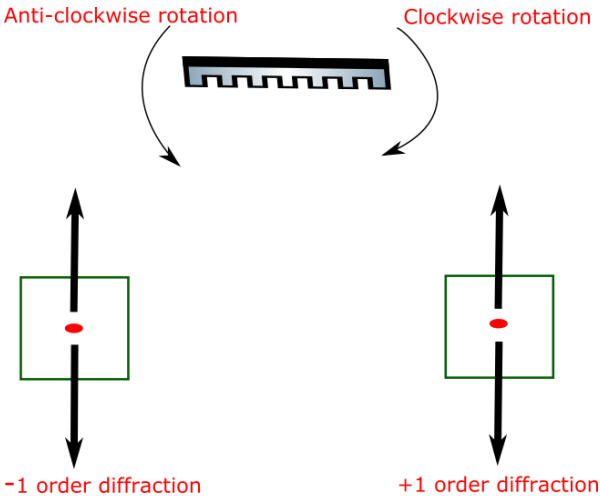


*Figure 10: Rotation of the grating sideways in clockwise and anti-clockwise direction.*

To understand Figure 10, imagine the grating placed in a position such that it gives +1 order reflection on your right hand side and the -1 order reflection on your left hand side. If the grating is rotated clockwise the +1 order reflection moves in downwards direction, whereas the -1 order reflection moves upwards. On the other hand, when the grating is rotated in anti-clockwise direction; the +1 order reflection moves upwards and -1 order reflection moves downwards. Thus, by rotating the grating all orders of refraction could be aligned at the same height. Figure 11 shows how rotating the grating affects a spectrum.

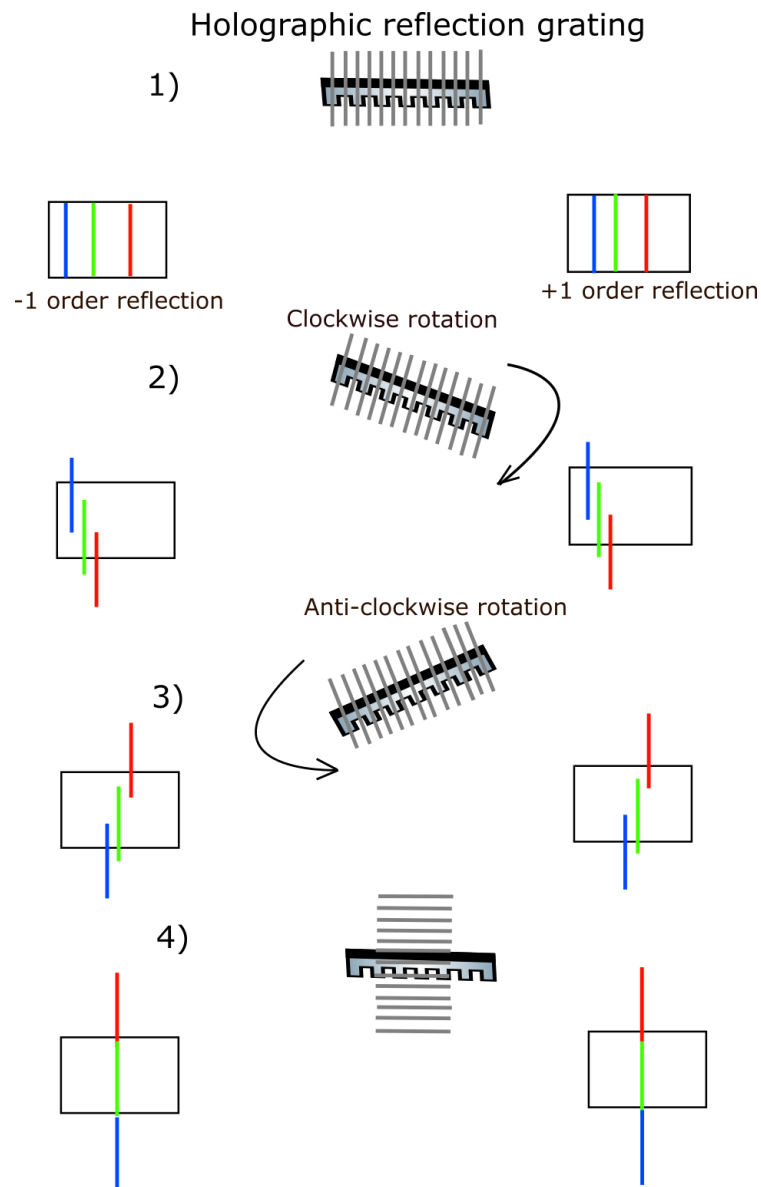


**Figure 11:** Effect of rotation of grating on spectral lines. 1) Holographic grating in vertical position with grating reflection lines oriented vertical gives spectral lines aligned at detector plane. 2) Rotating grating clockwise results in alignment of spectral lines downwards from blue to red. 3) Rotating grating anti-clockwise results in alignment of spectral lines downwards from red to blue. 4) Continuing rotating grating in anti-clockwise direction, until grating lines are horizontally oriented gives spectral lines one below the other but still vertical.

The rectangular box in each case in Figure 11 is the detector plane and shows how the spectral lines will appear in respective cases. Important to notice, that the orientation of the spectral lines always remained vertical, if the entrance slit is vertically orientated as it is the slit that is imaged onto the detector.

### 3.3 Recording spectrum with Periodic Shadowing

Figure 12 shows the spectrometer after being assembled, showing the position of the camera as well as the grating placed at the entrance slit for periodic shadowing.

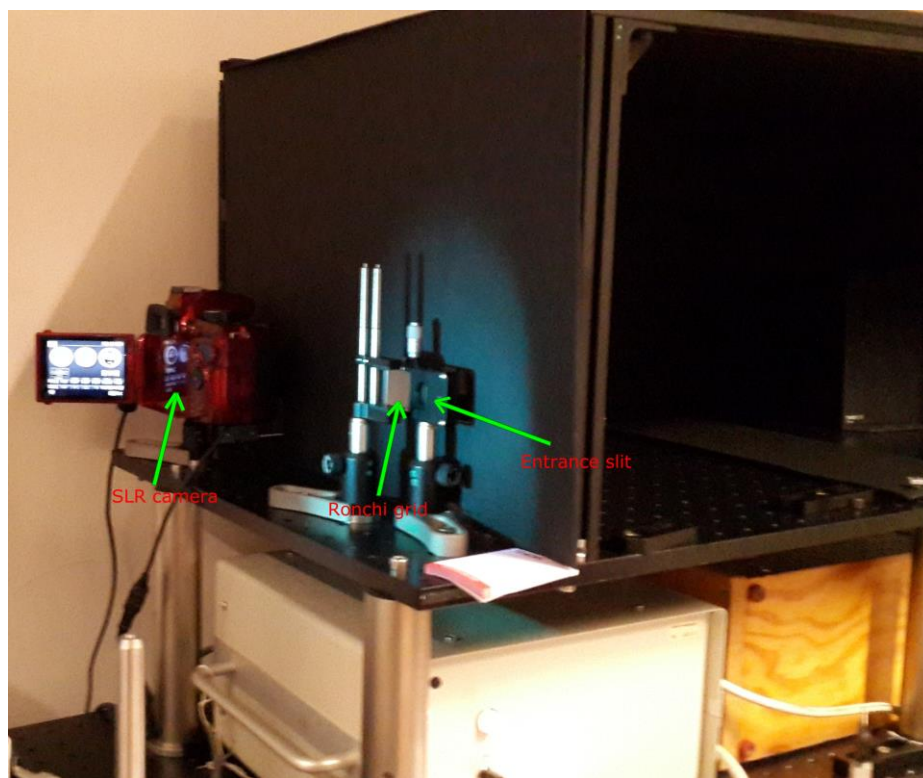


*Figure 12: Placement of the detector and Ronchi grid at the entrance slit.*

The spectral lines were captured in RGB scale by scanning the grating, shown in Figure 13. Notice how the spectral lines are spatially modulated. This is due to the grating at the entrance slit, casting periodic shadows onto the spectrum. By implementing a spatial lock-in algorithm on the acquired data, the stray light contribution is suppressed.



*Figure 13: Two captured pictures put together showing the spectral lines of +1 and -1 diffraction order with superimposed periodic shadows.*

The grating was mounted on a rotational stage, and the rotation is controlled via a motor which was mounted outside the spectrometer, shown in Figure 14. The rotation can be controlled using LabVIEW, as motor is connected to computer and also manually using switches on motor.

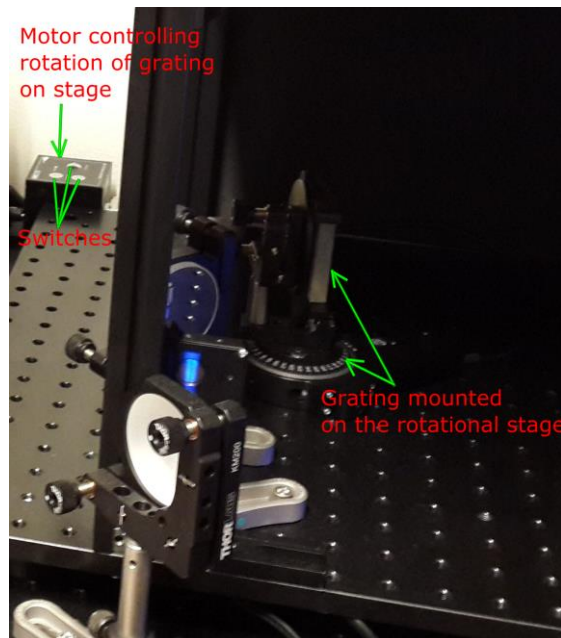


*Figure 14: Grating mounted on a rotational stage connected to a motor controlling the rotation.*



The spectrum was recorded by translating the rotational stage by from left most position (0 on scale) towards the right with an iteration of 0.2 mm step on its scale. An image was captured by the detector at each iteration step, recording in total 250 images. These images were merged together in MATLAB, by knowing the part of spectrum overlapped in each frame image to produce the final spectrum. The spectrum is seen in Figure 15, showing the intensity variation of the spectral peaks on the detector plane.

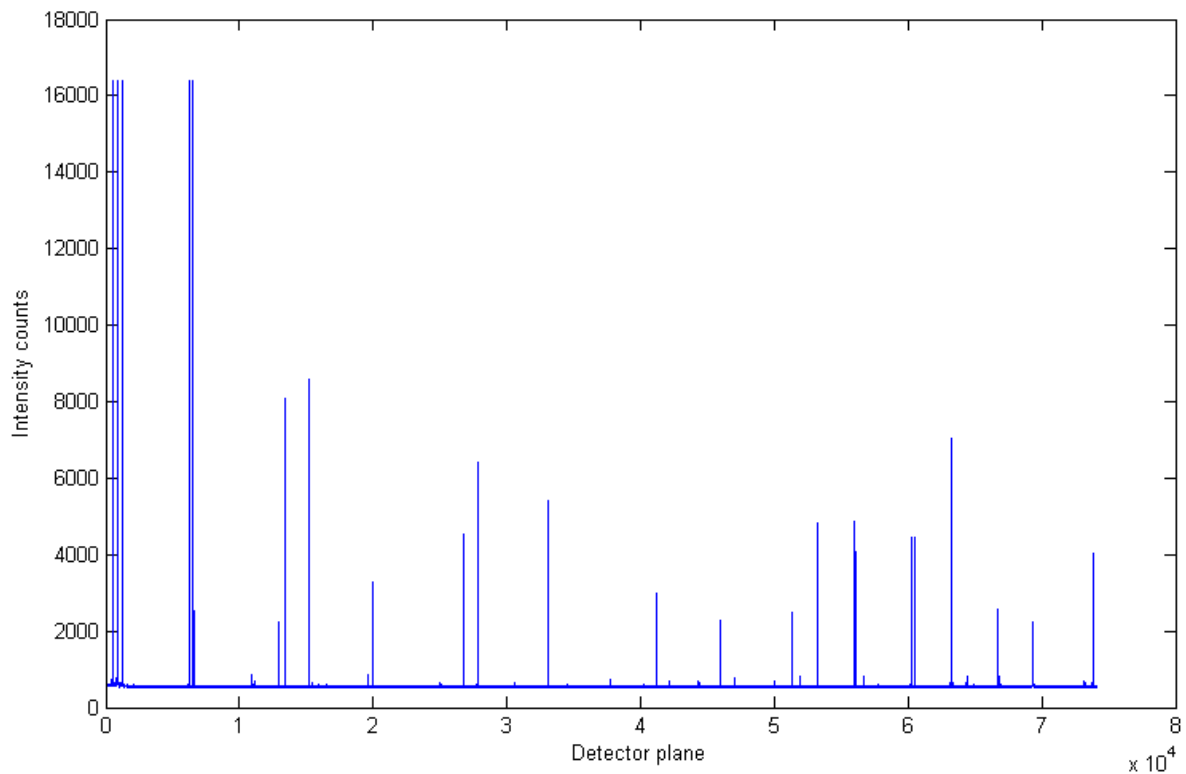


*Figure 15: Spectrum of Cadmium lamp, created by merging 250 individual spectra.*

Next step was to wavelength calibrate the spectrometer, achieved by matching the spectral peaks in Figure 15 with the spectrum of Cadmium lamp in the literature. This step can be performed in a more feasible manner; by employing CW laser sources of 3 or more different wavelengths.

### **3.4 Digital Micromirror Device (DMD) experiment to achieve High Dynamic Range Imaging**

This section involves all the problems encountered while incorporating the DMD into the spectrometer. The first step was to mount the DMD at the focus of the focusing mirror, such that the spectral lines reached the chip surface with a sharp focus. To handle and mount this device, it is recommended to avoid electrostatic discharge in order to prevent short circuits on the mainboard and thereby damaging the device.

#### **3.4.1 Tracing the ON and OFF state reflection and controlling a micromirror's flip**

Depending on the state of the DMD mirrors, spectral lines can be reflected in two directions. By uploading grayscale test images (8 bits) onto the DMD chip, these directions can be identified. An interesting observation was made and can be concluded as a fact that, depending upon the pixel value of the image uploaded onto the chip (ranging from 0 to 255), the rate of flip of mirrors is controlled. To verify this, two greyscale images were created; one was completely black (every pixel value 0) and the other was complete white (every pixel value 255). Now as expected, the incident lines were reflected only in one direction when either of them was uploaded. All the micromirrors flip to -12 degrees or +12 degrees, when a black or a white picture is uploaded respectively, and thereby reflecting the light in just one direction. Thus, a specific percentage of the incident light intensity can be reflected to the detector, and the remaining percentage can be reflected in the OFF state. The detector was placed in the reflection path of mirrors tilted in-12 degree position. For example, an image having a pixel value of half of 255 flips the corresponding micromirror for half of the time in ON state, and half of the time in OFF state; thus reflecting 50 % of the light onto the detector in a frame time, and 50 % in the other direction. Hence, if the pixel value is more towards the 255 (white scale), then more percentage is reflected in OFF state, and vice-versa. For example, a point of a spectral line having an intensity value of 90, will be reflected 64.71% to the detector side and 35.29 % in the OFF state.

#### **3.4.2 Experimental Challenges**

When the DMD was placed vertical and it was observed that a micromirror which was landed in the position of +12 degrees tilt reflected the incident light in upward direction and the one which was landed in -12 degrees tilt position reflected the rays downwards, see Figure 16. The DMD was mounted upside-down, and hence the -12 state reflections were monitored, going upwards onto the detector. To have both of the reflections lie in the same horizontal plane (same height level as the incident line), the device needs to be rotated by 45 degrees sideways, either in the clockwise or anti-clockwise direction.



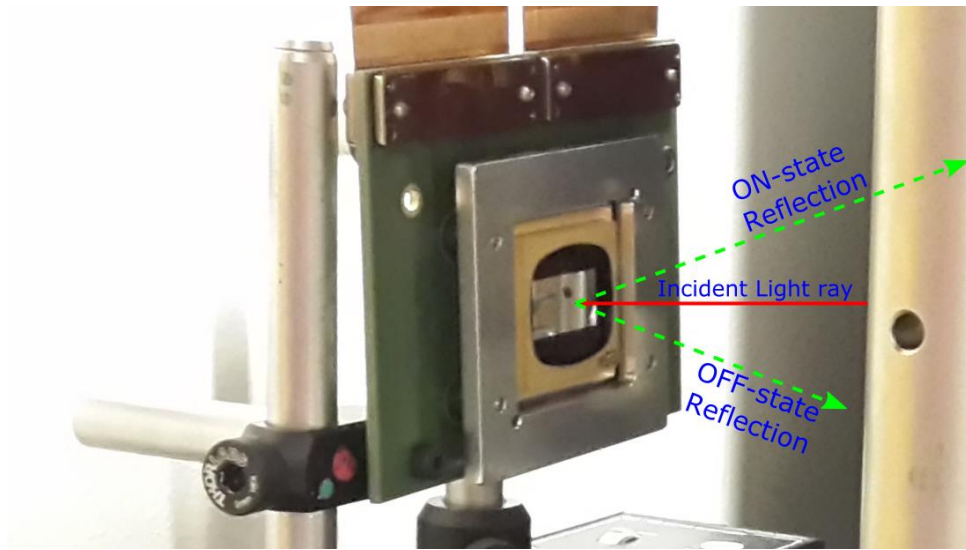


*Figure 16: DMD mounted vertically, reflects the incident light rays upwards and downwards for +12 and -12 micromirror tilt respectively.*

The device was rotated 45 degrees, and it was observed that the spectral lines were partly cut by the frame of the DMD, thereby reducing the spectral information being captured. Therefore, the DMD was kept vertical without any rotation, throughout the experiments. A solution to compensate for the reflections going in different heights could be the implementation of a dove prism, placed just before the DMD. A dove prism produces an inverted image of the incident light along longitudinal axis and has the ability to rotate an image. Using the dove prism would thus rotate the incident spectral lines by 45 degrees and hence compensate for the problem. Other solutions were, however, implemented in the current experimental setup.

The next step was to capture the reflection going upwards, which was challenging as the camera with an objective lens had to be tilted downwards to sharply image the DMD plane. When the camera was tilted downwards, then the device plane and the camera lens plane are no longer parallel and thus only a portion of the object plane could be focused. The imaging of the device plane was tried with close proximity that is by using a short focal length objective lens, but the camera objective blocked part of the signal.

Moreover, it was difficult to distinguish between the ON state and the OFF state reflection path. Even though all the mirrors were directing in OFF state, there was still some signal captured, but in principle the lines should have vanished. This occurs because the chip surface is highly reflective and works at small incident angles, such that the incident light and the two directions reflections have their paths in close proximity to each other in front of the device. It is required to have a longer optical path to separate them well. This problem was solved by implementing two right angled prisms and they were mounted together in configuration similar to a TIR prism [18] seen in Figures 1 and 17. The spectral lines were incident at an

angle greater than the critical angle (less than 45 degrees) and this caused the lines to be totally internally reflected by the prism onto the DMD chip surface. All the reflections that strike the prism boundary at an angle less than critical angle will pass and the rest will be totally internally reflected. The ON state reflection by the micromirror tilted at -12 degree passes through both prisms and is captured in the detector. The other state reflections strike at angle greater than the critical, and are totally internally reflected and exit at the same side as the incident light, seen in Figure 1.

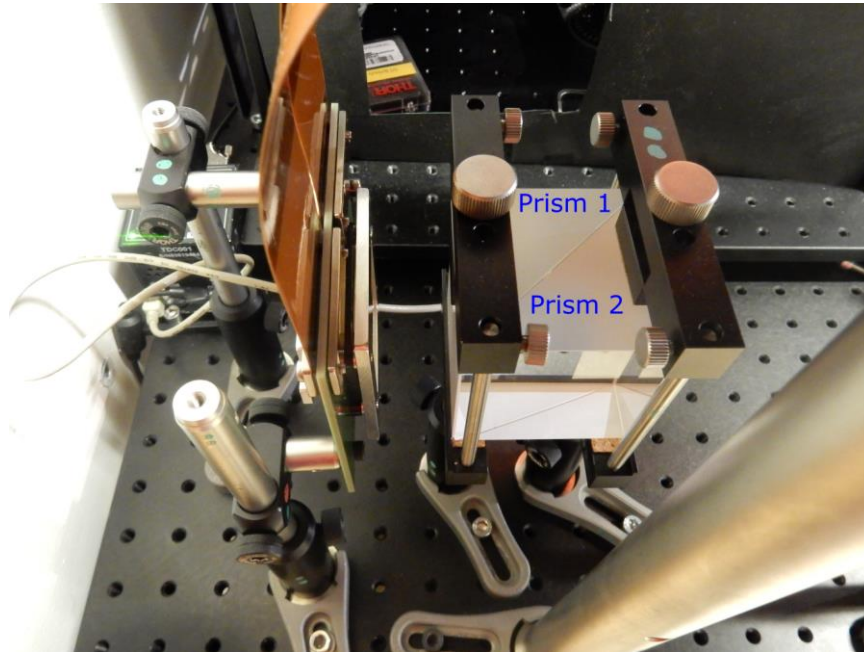
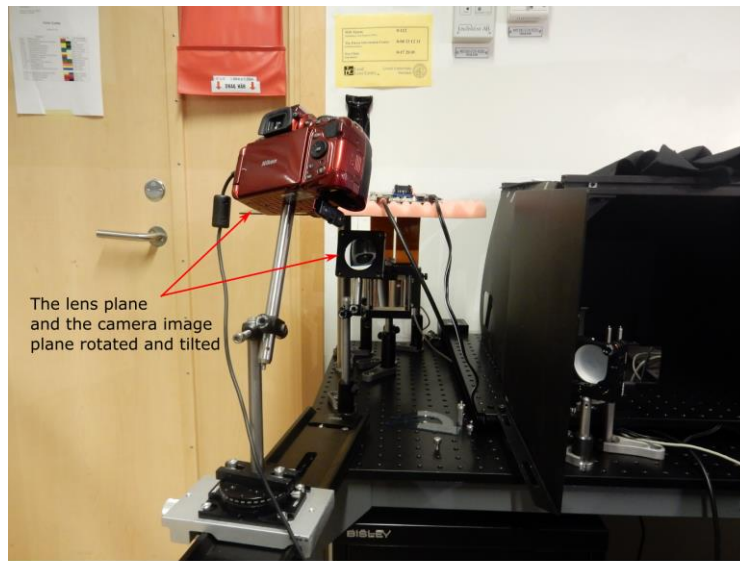
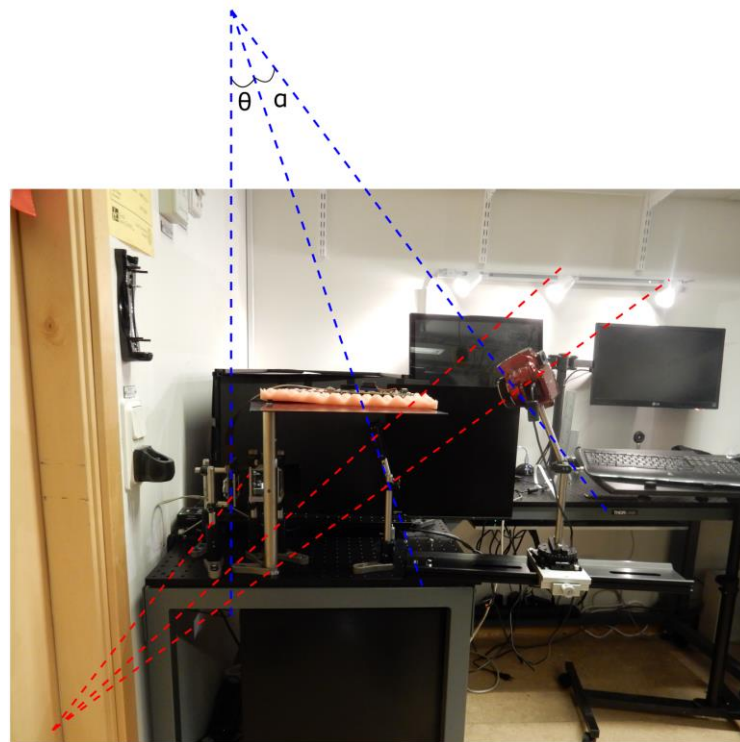


*Figure 17: Two right-angled prisms mounted together making a TIR prism design for separation of reflection paths.*

To deal with the problem of focusing the device plane and capturing the reflections going upwards, a Scheimpflug configuration, based on Scheimpflug principle was implemented, seen in Figure 18. To effectively obtain a sharp focus of the DMD plane, the tilting and the rotation of the lens plane and the camera sensor plane (without camera objective lens) is performed simultaneously. The mounting of the camera as it needs to be rotated, tilted and shifted along longitudinal axis simultaneously. This was achieved by mounting the camera on both a rotational stage and a translational stage, as well as using a holder that allowed the angle theta to be altered (see Figure 18). Based on equation (5), it was calculated that the camera sensor plane needed to be tilted 12 degrees with respect to the lens plane and at angle of 24 degrees with respect to the object plane. The three planes now met at a point, shown with the blue lines in Figure 18(b). To get the entire DMD in focus, the lateral reflection need to be addressed which was done by rotating the camera. The rotation for the camera sensor plane could be calculated using the equation (5); the angles are shown in Figure 18(b) with the red lines.



(a)



(b)

**Figure 18:** (a) Front view - The tilt and rotation of the lens plane and the camera image plane to capture reflections in focus by focusing the DMD plane. (b) The side view – The blue lines from left to right represent the vertical DMD plane axis, the tilted lens plane axis and the tilted camera image plane axis; all intersect at a point. The red lines from left to right represent the respective planes axis arising due to rotation of the respective planes; all intersect at a point.

## 4. Results & Discussions

### 4.1 Intensity control using the DMD

As explained before, depending upon the picture uploaded onto the DMD chip, the flipping of the mirrors can be controlled, in turn controlling the percentage of the incident light to be reflected onto the detector. A gray scale picture of a clown is uploaded onto the chip surface (see Figure 19). The spectral lines are incident on the surface and the reflections (in -12 degree tilt direction) are captured. Notice how a lower percentage of the line is reflected onto the camera from a whiter portion of the picture, and hence that part appears less intense, for example from the sclera (white part) in the eye. Similarly, a higher percentage of the line is captured when it is reflected from the darker portions of the picture and as a result that part is more intense, for example from the eyelashes and the black lining below the eye, shown in Figure 19. This illustrates how intensity by reflections is controlled using the DMD.



*Figure 19: The DMD chip surface uploaded with a gray scale picture of a clown reflects a lower percentage of the lines from whiter portion and vice-versa.*

## 4.2 HDR Image achieved with PS

The series of steps to achieve a HDR image with PS are described here.

1. A spectrum is recorded, titled as ‘original spectrum’, at a low exposure time (0.5 s) with a black picture (all pixels value is 0) uploaded onto the DMD. It can be seen that the left-most spectral line is the most intense amongst all and the right one is the least intense. The ratio of the most intense to the middle one is approximately equal to 2.5, whereas the ratio to the right one (least intense) is approximately equal to 3.5.

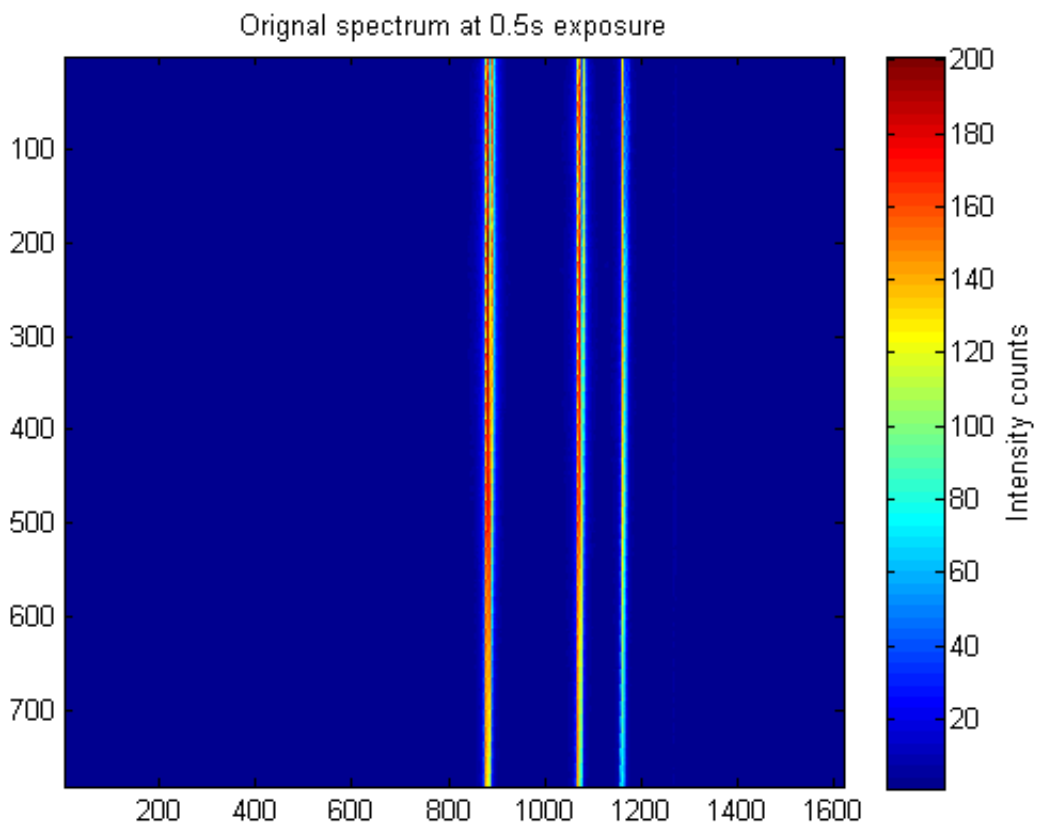


*Figure 20: A spectrum recorded at 0.5 s exposure time.*

2. The corresponding gray scale image of the original spectrum is uploaded onto the DMD, shown in Figure 21. The gray scale image on the DMD reflects a higher percentage of the intense line (the pixel value will be higher or more towards the white scale) in the OFF state and thus a lower percentage onto the detector. Similarly, for the less intense line in the original spectrum, the corresponding gray scale image on the DMD will reflect a higher percentage of it onto the camera.

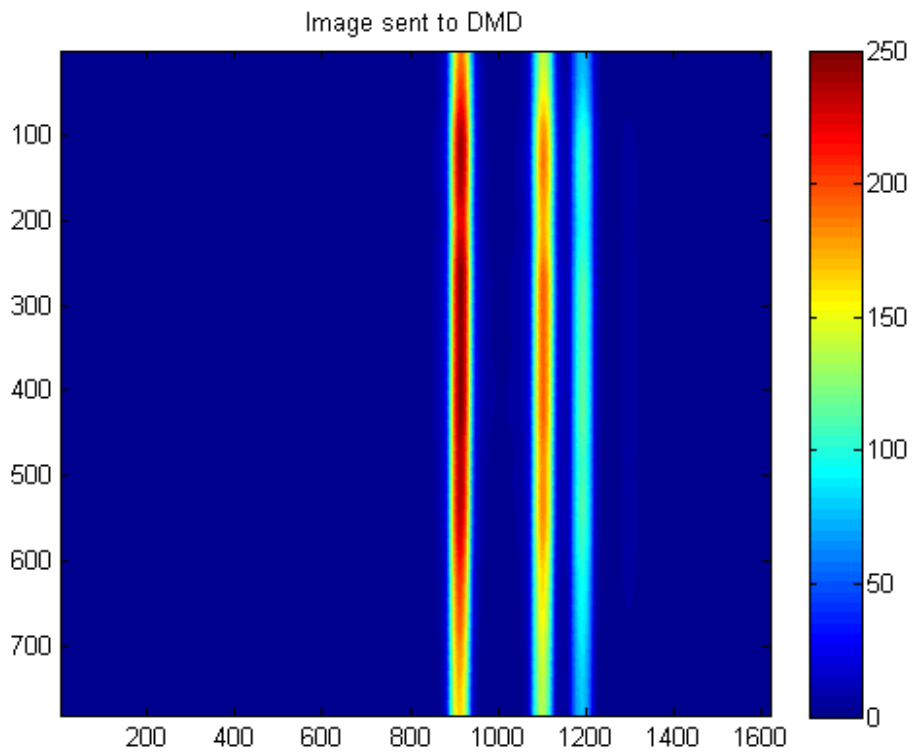


*Figure 21: The gray scale image of the original spectrum sent to the DMD.*

3. The spectrum is captured again with controlled reflections from the DMD; the most intense line is reflected the least and vice-versa. Notice how the three spectral lines are achieved of equivalent intensities.

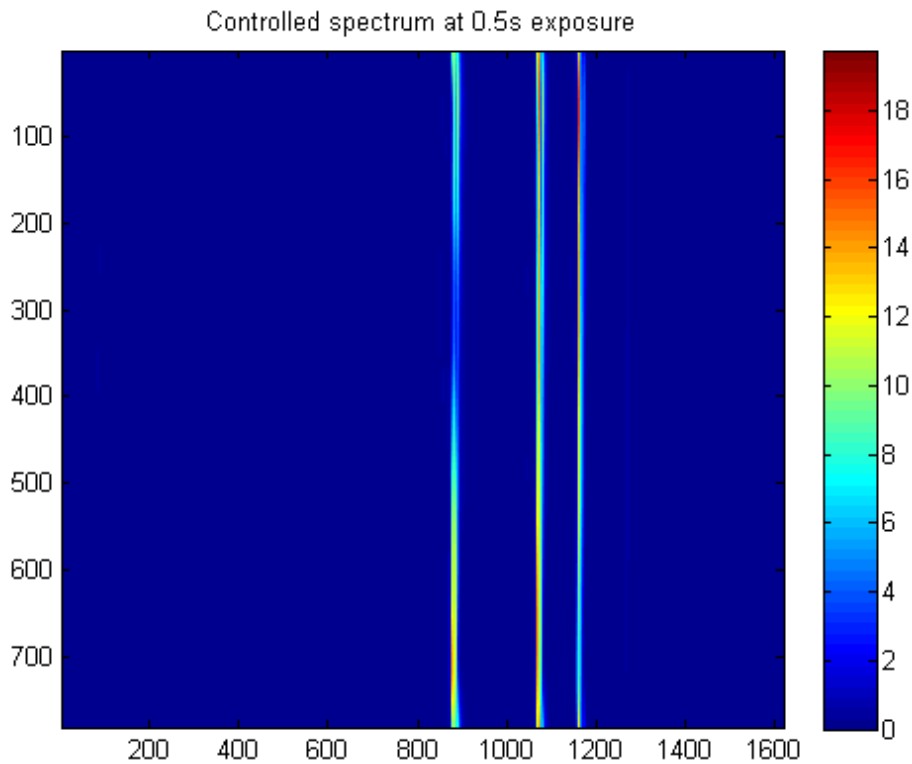


*Figure 22: Spectral lines of equivalent intensity obtained.*

- The exposure time is increased by 20 times (10 s) and the spectrum is captured again with the same gray scale image uploaded. In addition, the grid pattern is now positioned at the entrance slit, allowing the data to be analyzed using a lock-in algorithm, which suppresses the background stray light contribution. This is an essential step as the stray light contribution is significant at such long exposure time. Notice that now two very weak spectral lines can be observed without the intense spectral lines saturating the camera at such a long exposure time.

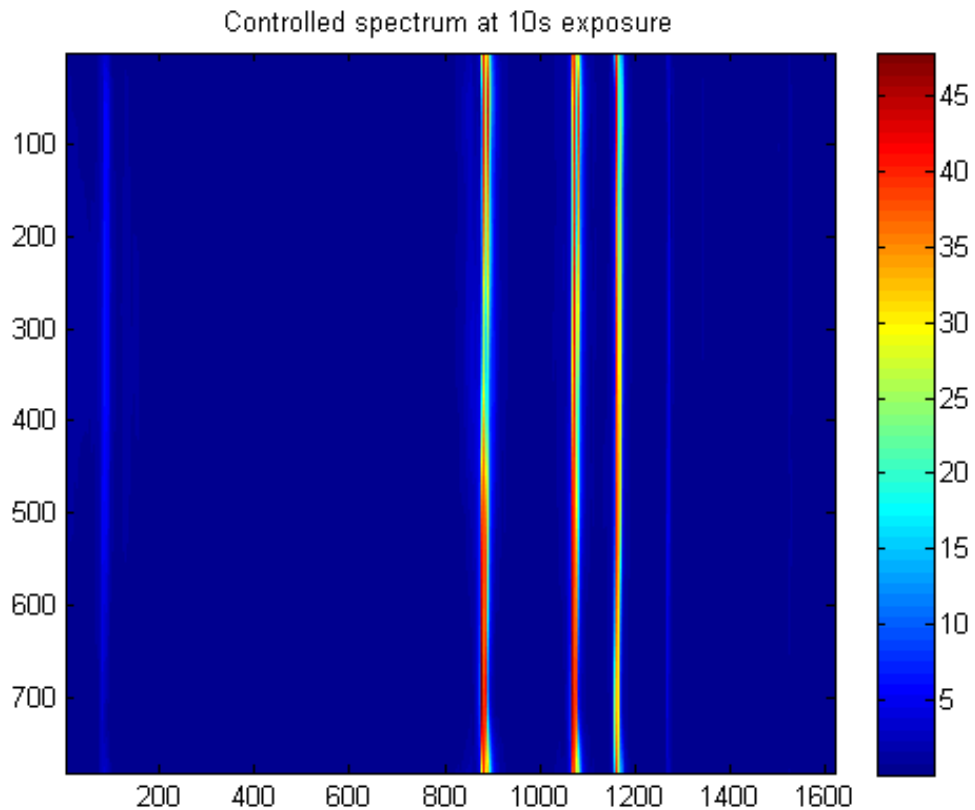


*Figure 23: Spectrum captured at 10s exposure time, also showing two additional weak spectral lines.*

- Next step is to produce the true spectrum from the controlled one, shown in Figure 24, achieved by multiplying the controlled spectrum obtained with the picture uploaded on the chip (to manipulate the spectrum), creating a HDR image at one exposure time and without saturating the camera.

The logarithmic plots in the Figure 25 highlight the difference between the original spectrum captured and the one captured using the described methodology. Here it can be seen that the HDR spectrum improves the signal-to-background value by more than an order of magnitude, revealing peaks that otherwise could not be observed.



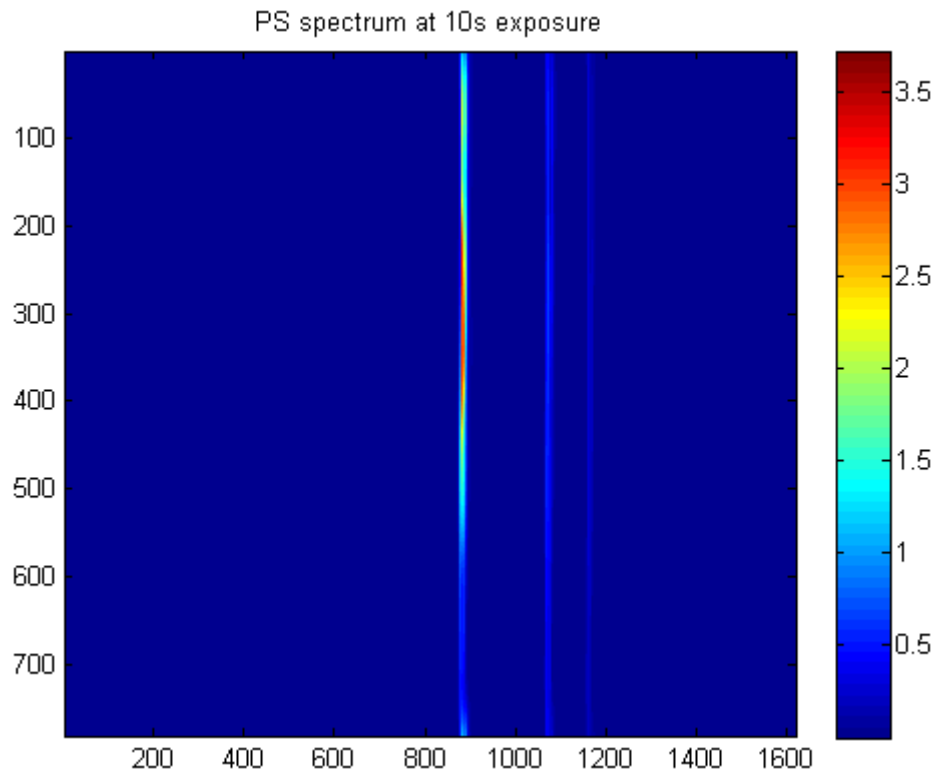


*Figure 24: True spectrum obtained at 10s exposure time with increased dynamic range.*

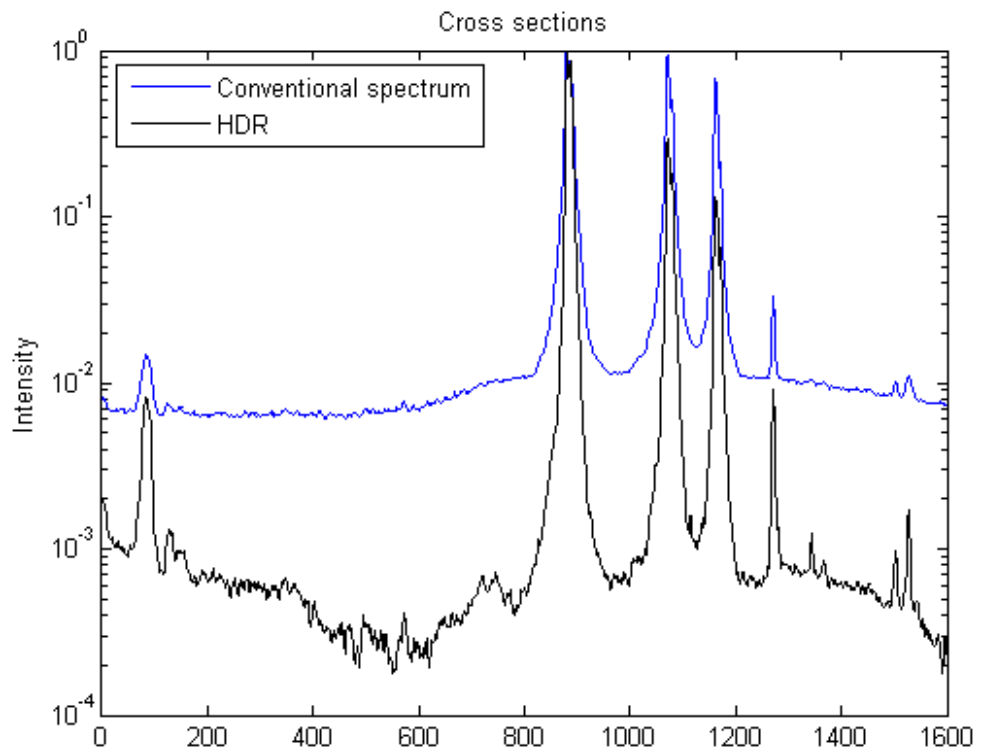


*Figure 25: Conventional spectrum and the increased dynamic range (HDR) spectrum.*



## 5. Conclusion and Outlook

In conclusion, a spectroscopic instrument, with a high dynamic range of imaging and having capabilities of suppressing stray light, has been developed and experimentally demonstrated. The dynamic range has been increased by a significant amount, with additional peaks resolved along with the presence of intense ones (seen in Figure 25), at one exposure time and without saturating the camera. Moreover, the background light is further suppressed using the technique PS. With the improved measurement accuracy, this instrument holds promise in many applications. For example, to assess the concentration of a chemical component present in a sample, absorption spectroscopy is used. This technique is based on quantifying the amount of radiation absorbed by a sample at a specific wavelength. Absorption troughs that are strong may prove difficult to quantify accurately due to the strong continuum. The developed DMD spectrometer may be of significant importance in such applications to make all spectral features proportional to each other.

Another typical spectroscopic application for this instrument is the Raman scattering spectroscopy, in which the intense laser lines (from inelastic scattering) makes it difficult to resolve the weak Raman scattering lines. The measurements from this spectroscopic technique currently suffer from both stray light and a limited dynamic range which can be improved using the designed instrument.

## References

1. Isao Noda, Yukihiro Ozaki. *Two-Dimensional Correlation Spectroscopy: Applications in Vibrational and Optical Spectroscopy*, (Wiley, 2004).
2. X. Qian, X. –H. Peng, D. O. Ansari, Q. Yin-Goen, G. Z. Chen, D. M. Shin, L. Yang, A. N. Young, M. D. Wang, and S. Nie, “In vivo tumor targeting and spectroscopic detection with surface-enhanced Raman nanoparticle tags,” *Nat. Biotechnol.* **26**(1), 83-90 (2008).
3. Elias Kristensson, Joakim Bood, Marcus Alden, Emil Nordström, Jiajian Zhu, Sven Huldt, Per-Erik Bengtsson, Hampus Nilsson, Edouard Berrocal, and Andreas Ehn. *Stray light suppression in spectroscopy using periodic shadowing*. *Optics Express*, Vol. 22, No. 7 (2014).
4. B. E. A Saleh, M. C. Teich. *FUNDAMENTALS OF PHOTONICS*, 2<sup>nd</sup> ed. (Wiley, 2007).
5. Sune Svanberg. *Atomic and Molecular Spectroscopy*, 4<sup>th</sup> ed. (Springer, 2004).
6. Hans Zappe. *Fundamentals of Mirco-Optics*, 1<sup>st</sup> ed. (Cambridge, 2010).
7. Ivan Pelant, Jan Valenta. *Luminescence Spectroscopy of Semiconductors*, 1<sup>st</sup> ed. (Oxford, 2012).
8. Robert B. J. Dorion. *BITEMARK EVIDENCE: A Color Atlas and Text*, 2<sup>nd</sup> ed. (2011).
9. Jeff Wignall. *Exposure Photo Workshop*, 2<sup>nd</sup> ed. (Wiley, 2011).
10. Larson, G.F., V.A. Fassel, R.K. Winge, and R. N. Kniseley, *Ultra-Trace Analyses by Optical Emission-Spectroscopy – Stray Light Problem*. *Applied Spectroscopy*, 1976. **30**(4), p. 384-391.
11. V. A. Fassel, J. M. Katzenberger, and R. K. Winge, “Effectiveness of interference filters for reduction of stray light effects in atomic emission spectrometry”, *Appl. Spectrosc.* **33**(1), 1-5 (1979).
12. P. W. J. M. Boumans. “A century of spectral interferences in atomic emission spectroscopy – Can we master them with modern apparatus and approaches?” *J. Anal. Chem.* **324**(5), 397-425 (1986).
13. S. Bykov, I. Lednev, A. Ianoul, A. Mikhonin, C. Munro, and S. A. Asher, “Steady-state and transient ultraviolet resonance Raman spectrometer for the 193-270 nm spectral range,” *Appl. Spectrosc.* **59**(12), 1541-1552 (2005).
14. Elias Kristensson, Andreas Ehn. *Improved Spectral Sensitivity by Combining Periodic Shadowing and High Dynamic Range Imaging*. (2015).
15. Alian Boutier. *Laser Velocimetry in Fluid Mechanics*, Chapter 6. (2012)
16. Liang Mei, Mikkel Brydegaard. *Atmospheric aerosol monitoring by an elastic Scheimpflug lidar system*. *Optics Express*, Vol. 23, No. 24 (2015).’
17. George Smith, David A. Atchison. *The eye and visual optical instruments*. (Cambridge, 1997).
18. Dan Dan, Ming Lei, Baoli Yao, Wen Wang, Martin Winterhalder, Andreas Zumbusch, Yujiao Qi, Liang Xia, Shaohui Yan, Yanglong Yang, Peng Gao, Tong Ye, Wei Zhao. *Dmd-based LED-illumination Super-resolution and optical sectioning microscopy*. Scientific report, *Nature* (2013).